G3: Genes|Genomes|Genetics Early Online, published on November 1, 2019 as doi:10.1534/g3.119.400349

Immune suppressive extracellular vesicle proteins of *Leptopilina heterotoma* are encoded in the wasp genome

Brian Wey[*‡], Mary Ellen Heavner[*†**], Kameron T. Wittmeyer[††], Thomas Briese[§], Keith R. Hopper[††], Shubha Govind[*†‡]

[*]Biology Department, The City College of New York, 160 Convent Avenue, New York, NY 10031, USA

† PhD Program in Biochemistry, The Graduate Center of the City University of New York, 365 Fifth Avenue, New York, NY 10016, USA

‡ PhD Program in Biology, The Graduate Center of the City University of New York, 365 Fifth Avenue, New York, NY 10016, USA

§ Center of Infection and Immunity, and Department of Epidemiology, Mailman School of Public Health, Columbia University, NY, NY 10032

**Laboratory of Host-Pathogen Biology, Rockefeller University, 1230 York Ave, New York, NY 10065

†† USDA-ARS, Beneficial Insect Introductions Research Unit, Newark, DE 19713

Short Title: *L*. *heterotoma* MSEV proteins are encoded in the genome

Key words: Extracellular vesicle, whole genome sequencing, *Leptopilina heterotoma*, endoparasitoid wasp, *Drosophila*, VLP, host-parasite, organelle, immune suppression

Corresponding Author:

Shubha Govind

160 Convent Avenue

Biology Department

The City College of New York

New York, New York, 10031

sgovind@ccny.cuny.edu

Phone number: 212-650-8571

BW ORCID: https://orcid.org/0000-0003-0895-5584

SG ORCID: https://orcid.org/0000-0002-6436-639X

ABSTRACT

Leptopilina heterotoma are obligate parasitoid wasps that develop in the body of their *Drosophila* hosts. During oviposition, female wasps introduce venom into the larval hosts' body cavity. The venom contains discrete, 300 nm-wide, mixed-strategy extracellular vesicles (MSEVs), until recently referred to as virus-like particles. While the crucial immune suppressive functions of *L. heterotoma* MSEVs have remained undisputed, their biotic nature and origin still remain controversial. In recent proteomics analyses of *L. heterotoma* MSEVs, we identified 161 proteins in three classes: conserved eukaryotic proteins, infection and immunity related proteins, and proteins without clear annotation. Here we report 246 additional proteins from the *L. heterotoma* MSEV proteome. An enrichment analysis of the entire proteome supports vesicular nature of these structures. Sequences for more than 90% of these proteins are present in the whole-body transcriptome. Sequencing and *de novo* assembly of the 460 Mb-sized *L. heterotoma* genome revealed 90% of MSEV proteins have coding regions within the genomic scaffolds. Altogether, these results explain the stable association of MSEVs with their wasps, and like other wasp structures, their vertical inheritance. While our results do not rule out a viral origin of MSEVs, they suggest that a similar strategy for co-opting cellular machinery for immune suppression may be shared by other wasps to gain advantage over their hosts. These results are relevant to our understanding of the evolution of figitid and related wasp species.

INTRODUCTION

Parasitic wasps are amongst the most abundant insects; they are vital to biodiversity and contribute to biological control of agricultural pests (Narendran 2001; Rodriguez et al. 2013). A common strategy for reproductive success of parasitic wasps is suppression of immunity in their larval hosts. Parasitic wasps produce viruses or virus-like particles in tissues associated with the ovary. Wasps of the Ichneumonoidea superfamily produce symbiotic polydnaviruses (PDVs), which package circular dsDNA. PDV (Bracovirus (BV) in braconid wasps; Ichnovirus (IV) in ichneumonid wasps) genomes are integrated within the wasp genome as islands of viral genes. Upon oviposition, PDVs suppress host immunity. BVs and IVs derive from nudivirus and large DNA cytoplasmic viruses, respectively (reviewed in (Strand and Burke 2015; Drezen et al. 2017; Gauthier et al. 2018) and references therein).

Immune-suppressive virus-like particles (VLPs) (e.g., VcVLPs in the ichneumonid *Venturia canescens* and FaENVs in the braconid *Fopius arisanus*) lack proviral DNA segments, but are of viral origin and transfer virulence proteins into host cells (Pichon et al. 2015; Burke et al. 2018). Viral genes encoding VLP proteins are either dispersed in the wasp genome (as in VcVLP) or present in discrete genomic areas (as in FaENV). Thus, various independent viral endogenization events have been important for successful parasitism by these wasps (Strand and Burke 2015; Gauthier et al. 2018).

Here, we focus on immune-suppressive particles of figitid wasps of the genus *Leptopilina,* that infect *Drosophila* spp. and are gaining importance as models for natural host-parasite interactions (Keebaugh and Schlenke 2014). *Leptopilina heterotoma* (*Lh*), *L. victoriae* (*Lv*), and *L. boulardi* (*Lb*) produce VLPs in their venom glands. The VLPs of

Leptopilina spp. and their proteins have been linked to parasite success (Rizki et al. 1990; Dupas et al. 1996; Morales et al. 2005; Labrosse et al. 2005; Chiu et al. 2006; Heavner et al. 2014). Evidence for DNA in *Leptopilina* VLPs is lacking, and because of the absence of a published wasp genome, the chromosomal versus extrachromosomal location of MSEV protein genes is not known. Our goals here are (a) to describe additional proteins in the MSEV proteome and examine their relationship with PDV and other viral proteins, and (b) determine whether MSEV genes are encoded within the wasp genome.

We recently described 161 proteins in the VLPs from two *Lh* strains in three classes: conserved eukaryotic with cellular function (Class 1), infection- and immunity-related (Class 2), and unannotated (novel) proteins without similarity to known proteins (Class 3) (Heavner et al. 2017). Class 1 proteins include several vesicular transport and endomembrane system proteins. Class 2 proteins include predicted modulators of immune response, e.g., metalloendopeptidases, RhoGAPs, a knottin-like protein, and a new family of prokaryotic-like GTPases whose genes lack introns. A striking example of Class 3 proteins is p40, with three-dimensional structural similarity to Type 3 secretion system (T3SS) needle tip proteins, IpaD/SipD/BipD from Gram-negative bacteria, *Salmonella, Shigella* and *Burkholderia*. Earlier results have indicated that the *p40* gene (unlike the *GTPase* genes) is expected to have introns. These results suggested that *Lh* VLPs have novel properties with elements of the prokaryotic and eukaryotic secretion systems and possess a functionally diverse array of immune-suppressive proteins. We therefore renamed VLPs as Mixed Strategy Extracellular Vesicles (MSEVs). Their variable morphologies distinguish them from ordered PDV morphologies. Additionally,

genes encoding abundant MSEV proteins p40 and GTPase are present even in antibiotic-treated wasps. These results favored a non-microbial nature of MSEVs (Heavner et al. 2017).

Here, we present an analysis of an additional 246 proteins from the *Lh* 14 MSEV proteome to obtain a more comprehensive description. A combined analysis of these and previous results reinforce the idea that the MSEV proteome is enriched in exosomal proteins and that Class 3 proteins are not shared with either *Lb* or an unrelated *Ganaspis* spp. Whole-body transcriptome of adult *Lh* wasps validated the expression of the MSEV genes. *De novo* genomic assembly and analyses revealed 90% of conserved Insecta Benchmarking Universal Single-Copy Orthologs (BUSCOs), as well as a majority (375/407; ~90%) of the MSEV proteins are encoded in the wasp genome. While we cannot rule out a viral origin of MSEVs, in aggregate, our results provide a clearer understanding of the extant nature of these complex structures and strengthen the idea that specialized extracellular vesicles transfer wasp virulence factors and other parasite proteins into *Drosophila* host cells.

MATERIALS AND METHODS

Insects: Isogenized *Lh* strains New York (NY; (Chiu and Govind 2002; Chiu et al. 2006)) and *Lh* 14 (Schlenke et al. 2007), were raised on the *y w* strain of *D. melanogaster* that were reared on standard cornmeal, yeast, and agar fly food at 25°C as described (Small et al. 2012). Adult wasps were collected from parasitized hosts, 25 days after infection at 25ºC. Male and female wasps were stored on fly food with 70% honey on "buzz" plugs.

Analysis of MSEV super-set ORFs: Previously undescribed open reading frames (ORFs) from the *Lh* 14 MSEV proteome and sequenced as part of (Heavner et al. 2017) (PXD005632) are analyzed in the context of the published female abdominal (Goecks et al. 2013) and whole body (this study) *Lh* 14 transcriptomes. We have not observed any difference in venom activities of *Lh* 14 and *Lh* NY (Morales et al. 2005; Schlenke et al. 2007), or in wasp success under laboratory conditions. The *Lh* 14 ORFs were aligned against transcripts from BioProject: PRJNA202370, Accession number GAJC0000000 (Goecks et al. 2013) as previously described in (Heavner et al. 2017). Proteins with an ORF and a transcript were run through the BLAST2GO (v 5.2; downloaded June 2018) annotation pipeline with an E-value threshold of $1x10^{-7}$ (Conesa et al. 2005; Götz et al. 2008). Results were organized and classified based on Gene Ontology (GO) terms from UniProt and InterPro (Ashburner et al. 2000; Jones et al. 2014; Consortium 2015; Carbon et al. 2019). Proteins were considered "virulence-related" based on GO terms indicating involvement with infection, host evasion, inflammation, and immune response. ORFs that did not return results via BLAST or InterProScan (Class 3

proteins) were run through Conserved Domain Search (CDD) on NCBI (version 3.16) (Marchler-Bauer et al. 2017). The E-value cut off for CDD search was $1x10^{-2}$. Proteins were considered to have a signal peptide if one was predicted using Phobeus and Signal P (Kall et al. 2004; Kall et al. 2007; Nielsen 2017; Almagro Armenteros et al. 2019). Transmembrane domains were considered to be present if they were predicted using Phobeus and TMHMM (Sonnhammer et al. 1998; Krogh et al. 2001; Kall et al. 2004; Kall et al. 2007).

The GhostKOALA algorithm (Kanehisa et al. 2016) was used to assign KEGG ortholog (KO) numbers for the MSEV superset protein sequences. If a primary KO number failed to be assigned by GhostKOALA, a secondary number assignment with a score >= 50 was used. Redundant KO numbers were excluded.

MSEV proteins were included in the enrichment analyses only if a human ortholog exists; the gene identifiers for human orthologs were obtained from the MSEV KO and the UniProt mapping utility (Li et al. 2015; Consortium 2015). (Human orthologs were chosen because a robust proportion of Vesiclepedia's data is derived from human vesicle proteomes.) The orthologs of human genes were analyzed for enrichment with the FunRich algorithm (Pathan et al. 2015; Pathan et al. 2017) against the Vesiclepedia database (Kalra et al. 2012; Pathan et al. 2019).

Finally, the MSEV proteome was used as a query using BLASTp for the following databases: "non-redundant" (nr), nr restricted to Taxid: Viridae (10239), nr restricted to Taxid: Polydnaviridae (10482), and nr restricted to Taxid: Unclassified Polydnaviridae (40273) (E-value threshold: $1.0x10^{-3}$, %ID minimum: 20%, performed 04/16/2019). tBLASTn of *L. boulardi* and *G. hookeri* (previously called *Ganaspis spp. 1*) (Goecks et

158 al. 2013) transcriptomes was performed on 03/10/2019; the threshold for homologs in
159 *Lb* and *G. hookeri* were 25% ID and an E-value of $1.0x10^{-10}$.
160
161 **Genomes sequencing and assembly:** Library preparations, sequencing reactions,
162 and associated validations were conducted by GENEWIZ, Inc. (South Plainfield, NJ,
163 USA). Genomic DNA was extracted from ~50 mg of tissue (~100 wasps) of *Lh* males
164 and females separately using mixed bead beating and PureLink Genomic DNA
165 extraction kits following manufacturer's protocol. Quantification of extracted DNA was
166 performed using Nanodrop and Qubit2.0 Fluorometer (Live Technologies, Carlsbad,
167 CA, USA). Integrity of genomic DNA was verified by gel electrophoresis (0.6% agarose).
168 DNA libraries were prepared for each wasp gender by acoustic shearing fragmentation
169 using a Covaris S220. Fragments were end repaired and adenylated prior to adapter
170 ligation on 3' ends (NEB NextUltra DNA Library Preparation kit, Illumina, San Diego,
171 CA, USA). Enrichment and indexing of adapter-ligated DNA was done through limited
172 cycle PCR. DNA library validation was performed using TapeStation (Agilent
173 Technologies, Palo Alto, CA, USA). Libraries were quantified using Qubit 2.0
174 Fluorometer.
175 Real time PCR (Applied Biosystems, Carlsbad, CA, USA) was used to quantify
176 DNA molar mass for each library before multiplexing in equal molar mass. DNA libraries
177 were sequenced using a 2x150 paired-end (PE) configuration on one lane on an
178 Illumina HiSeq 4000. Image analysis and base calling were performed using the HiSeq
179 Control Software (HCS) on the HiSeq instrument.

The average size of inserts (without adaptors) in the Illumina library was ~300-350 bp. *De novo* assembly of reads and scaffolding of contigs was performed using ABySS 2.2 (Jackman et al. 2017) by the New York Genome Center. *De novo* assembly of combined male/female genome was performed using Platanus-allee (Kajitani et al. 2019) and scaffolding was improved using AGOUTI (Zhang et al. 2016) on the University of Delaware's BIOMIX cluster.

Sequences from *Drosophila*-associated bacteria such as *Wolbachia* spp., *Acetobacter pasteurianus,* and *Lactobacillus plantarum* were identified in both assemblies. *Wolbachia* are endosymbionts of many insects including *Leptopilina* spp. (Pannebakker et al. 2004; Werren et al. 2008; Gueguen et al. 2012). *Lactobacilli* and *Acetobacter* are symbionts and commensals of sugar-consuming insects (Crotti et al. 2010; Engel and Moran 2013). Among the three bacterial species, *Wolbachia* sequences were the most abundant. BLASTx analysis showed that predicted genes from *Wolbachia* scaffolds were associated with *Wolbachia* proteins in GenBank. These bacterial and mitochondrial sequence-containing scaffolds were identified during the NCBI submission process and were manually removed from the submission.

Evaluation of genome assemblies: Assemblies made with ABySS and Platanus-allee with AGOUTI were run through QUAST v4.0 (Mikheenko et al. 2016) to determine scaffold number, N50, and GC%. All assemblies were examined for conserved genes and orthologs with BUSCO v9 (Simão et al. 2015; Waterhouse et al. 2017) using the Insecta set and training parameters set to "Nasonia". NCBI BLAST+ (v 2.7.1) was used to compare select scaffolds produced from male and female genome assemblies

(Johnson et al. 2008; Camacho et al. 2009). E-value threshold was set at $1x10^{-7}$. E-values of alignments were considered acceptable if within the range of 0 to $1x10^{-10}$.

K-mer analysis was performed using the K-mer Analysis Toolkit (KAT) (Mapleson et al. 2016) and heat maps were used to compare multiplicity (coverage plus repeats) of K-mers to GC content of the reads, coloring bins according to the number of distinct K-mers in each. This analysis was used to determine whether there were separate clusters of multiplicity/GC content that might arise from different sources, such as contamination. BLAST (Altschul et al. 1990; Camacho et al. 2009; Johnson et al. 2008) was used to search for homologs of a random sample of genomic scaffolds to which reads from each cluster mapped. The joint assembly of the *Lh 14* genome was compared to the published *L. clavipes* genome (Bioproject: PRJNA84205 (Kraaijeveld et al. 2016)) through maps of 27-mer multiplicity versus GC content. Finally, 27-mer multiplicity/GC content of the scaffolds (9.6 Mb) containing MSEV genes was compared to a random subset of scaffolds (9.6 Mb) without MSEV genes. Statistical differences between *Lh 14* and *L. clavipes* genomes and between MSEV-gene containing scaffolds and non-MSEV-gene containing scaffolds were calculated using a multivariate Cramér test (Ihaka and Gentleman 1996; Baringhaus and Franz 2004; Franz 2019).

Gene predictions, gene annotation, and viral gene searches: Gene predictions were performed on parallel and anti-parallel strands using AUGUSTUS (v3.3.1; August 2018) (Stanke et al. 2004; Stanke and Morgenstern 2005; Keller et al. 2011) with the *Nasonia* training set. The AUGUSTUS readout was separated into mRNA, coding DNA sequence (CDS), and translations by gffread (Trapnell et al. 2012).

Gene predictions were annotated by performing a BLASTx of all gene predictions against the entire nr database (Downloaded on January, 2019) and InterProScan on the University of Delaware BIOMIX Cluster before using BLAST2GO (Conesa et al. 2005; Götz et al. 2008) to finish annotation based on BLASTx and InterProScan results.

NCBI BLAST+ (v 2.7.1) was used on a local machine to search predictions and scaffolds, cutoff was %ID >70%, E-value < 1E-50, and query coverage > 70%. MSEV genes and $1x10^{-2}$ for Polydnavirus and Nudivirus proteins. Family *Polydnaviridae* and *Nudiviridae* protein sequences for the 11 species available on OrthoDB v9 were downloaded on February 2019 (Johnson et al. 2008; Camacho et al. 2009).

Whole-body transcriptome sequencing and assembly: Total RNA extraction, library preparations, sequencing reactions, and bioinformatics analysis were conducted at GENEWIZ, INC (South Plainfield, NJ, USA). RNA was extracted from frozen tissue with the Qiagen RNeasy Plus Universal mini kit using manufacturer's instructions (Qiagen, Hilden, Germany). The extracted RNA was quantified using a Qubit 2.0 Fluorometer and its integrity was checked with the 4200 TapeStation (Agilent Technologies, Palo Alto, CA, USA).

RNA samples were enriched for mRNA using Oligo d(T) beads. RNA sequencing libraries were prepared using the NEBNext Ultra RNA Library Prep Kit for Illumina following manufacturer's instructions (NEB, Ipswich, MA, USA). The sequencing libraries were validated by using the Agilent TapeStation. Quantification was performed using the Qubit 2.0 Fluorometer and quantitative PCR (KAPA Biosystems, Wilimington, MA, USA).

Sequencing libraries were clustered on a single lane of a flow cell and sequenced on the Illumina HiSeq 4000 instrument using a 2x150 PE configuration. Image analysis and base calling were conducted by the HCS. Raw sequence data (.bcl files) was converted into fastq files and de-multiplexed using Illumina's bcl2fastq 2.17 software. One mismatch was allowed for index sequence identification.

The Trinity v2.5 (Grabherr et al. 2011), *de novo* assembler was used to assemble the *Lh 14* transcripts. The *de novo* assembled transcriptome was created with a minimum contig length of 200 bp per sample. Transrate v1.0.3 (Smith-Unna et al. 2016) was used to generate statistics for the *de novo* assembled transcriptome. EMBOSS tools getorf were then used to find the ORFs within the *de novo* assembled transcriptome. The *de novo* transcriptome assembly was then annotated using Diamond BLASTx (Buchfink et al. 2015).

The transcriptome reads were mapped to the genomic scaffolds for downstream analyses using HISAT2 or BWA (Li and Durbin 2009; Kim et al. 2015).

Preparation of template DNA and PCR: Male and female wasps (n=12, for each sex), were separated and washed in 70% ethanol, and then rinsed twice in deionized water. Genomic DNA (gDNA) was extracted using a Qiagen DNeasy Blood and Tissue kit following provided protocols. gDNA was eluted in Tris-EDTA buffer, pH 8.0, and stored at 4°C. The concentration of gDNA was determined by NanoDrop (Thermo Fisher).

For cDNA preparation, male and female wasps (n=12 for each sex), were separated and washed in 70% ethanol and rinsed twice in deionized water. Total body RNA was extracted using 100 µL of Trizol (Invitrogen) following manufacturer's

protocols. RNA was resuspended in 0.1% DEPC treated water and treated with DNase I to remove contaminating DNA (Thermo Fisher Scientific). The RNA concentration was determined by NanoDrop (Thermo Fisher). cDNA was synthesized using Proto-Script First Strand cDNA Synthesis Kit (New England Biolabs).

Analysis of select genes: Primers for *p40 and SmGTPase01* are as follows:

p40 forward: GAATCATTGTTCGTTTGCTTGAAGAAAGAATTGG

p40 reverse: CATTATTAATGGGCCTTTACAATAATTTTAGCC

SmGTPase01 forward: CGTTGCACTACCTTGTTTGTCA

SmGTPase01 reverse: TTGTCTTTGCCCTGAGCGTT

PCRs were performed with Taq polymerase (gift of C. Li lab, CCNY), PCR buffer (300 mM Tris HCl pH 9.5, 75 mM $(NH_4)_2SO_4$, 10 mM $MgCl_2$) and deoxyribonucleotides (0.2 mM; Thermo Fisher Scientific). The PCR products were resolved on a 1% agarose gel in Tris acetic acid EDTA buffer (40 mM Tris HCl pH 7.6, 20 mM acetic acid, 1mM EDTA pH 8.0). Ethidium bromide (Sigma Aldrich)-stained gels were visualized on an ultra violet Trans-Illuminator (UVP) and gel images were taken using the DigiDocIt Imaging System (UVP). Gel images were processed in Adobe Photoshop for clarity only.

gDNA or cDNA-containing PCR products were cloned into pCR TOPO II plasmids (Invitrogen) and transformed into DH10β competent cells (New England Biolabs). For plasmid preparation, colonies were screened via PCR and positive

293 colonies were cultured in Luria Broth with ampicillin (100 µg/mL) at 37°C overnight.
294 Plasmids were extracted using Plasmid Miniprep kit (Qiagen) and sequenced
295 (GENEWIZ, INC. South Plainfield, NJ, USA). Sequences were aligned using NCBI
296 BLAST+ (Johnson et al. 2008; Camacho et al. 2009) and Clustal Omega (Li et al. 2015).
297 Expected PCR band sizes were determined using SerialCloner (v2.6.1).
298
299 **Data availability:** *L. heterotoma* strains (Chiu et al. 2006; Schlenke et al. 2007) are
300 available upon request. All supplemental files and figures can be downloaded from
301 figshare (https://figshare.com/s/3a4598308909307c2ae0). File S1 contains details of
302 supplemental files and tables. File S2 contains listing of accession numbers for all
303 sequences reported in this work. Figure S1 contains the 27-mer vs GC count
304 comparison of MSEV containing scaffolds to non-MSEV containing scaffolds. Table S1
305 contains annotations and related data for proteins. Table S2 contains BLAST search
306 results of the MSEV proteome against the nr database. Table S3 contains all BUSCOs
307 found in male, female, and joint genome assemblies. MSEV protein sequences are
308 available upon request. Accession numbers for datasets are as follows: *Leptopilina*
309 *heterotoma* strain *Lh* 14, genome assembly: Male genome: QYUB0000000, Female
310 genome: QYUC0000000, Joint genome: VOOK00000000. *Leptopilina heterotoma* strain
311 *Lh* 14, whole-body transcriptome: GHUQ00000000. *Leptopilina heterotoma* abdominal
312 transcriptome by Goecks et al.: GAJC0000000. *Leptopilina clavipes* genome Bioproject:
313 PRJNA84205. *Leptopilina heterotoma* strain *Lh* 14 proteome: PRIDE: PXD005632

RESULTS AND DISCUSSION

The MSEV proteome superset: A comparative study of the proteomes of the MSEVs from *Lh* 14 and *Lh* NY strains previously generated a list of 161 “common” MSEV proteins (Heavner et al. 2017). More than 90% of the 161 proteins are part of the *Lh* 14 MSEV proteome. To describe MSEVs more completely, we characterized a larger set of 407 MSEV proteins from *Lh* 14 (161 common and 246 *Lh* 14) and define this set as the *Lh* MSEV “super-set” (Fig. 1A). Key results from annotation-based classification, analysis for signal peptide and/or transmembrane domain, and presence/absence of proteins in related wasps are summarized below and in Table S1.

The presence/absence of signal peptide (SP) alone, or SP with/without the transmembrane (TM) domain(s) in MSEV proteins reveals their possible location (i.e., potentially secreted into the venom gland lumen or associated with MSEV membrane). We therefore searched the 246 *Lh* 14 proteins for SP and TM domains. Of the 246 proteins, 55 (22.35%) have a predicted SP domain, 37 (15.04%) have a predicted TM domain, while 6 (2.44%) have both a predicted SP and TM domain.

After annotation, we found that a majority (183/246 or 74.39%) of the 246 proteins can be classified as core eukaryotic cell biology proteins (Class 1); 13/246 (5.28%) proteins as virulence- and immunity-related based on associated GO terms (Ashburner et al. 2000; Carbon et al. 2019) (Class 2); and 50/246 or 20.32 % as novel sequences without high confidence annotation (Class 3) (Table S1). A presence/absence analysis of these 246 proteins in published transcriptomes (Goecks et al. 2013) of *Lb* or a more distantly related wasp, *G. hookeri* (for thresholds see Methods) revealed the following: only 43/246 (17.47%) *Lh* MSEV proteins are expected

to be found in *Lb* and/or *G. hookeri* (Table S1). Of these, 33/43 (76.74%) proteins were in Class 1 but only 7/43 (16.27%) and 3/43 (6.98%) were in Class 2 and Class 3 categories, respectively. These results support the idea that, multiple but different, infection strategies and/or host evasion strategies might exist among different wasps infecting the same hosts.

While most of the Class 1 proteins were annotated as ribosomal or mitochondrial-related, a few were described as integral membrane proteins, vesicle trafficking protein SEC22b (E-value: 6.22E-145), and the ion channels sideroflexin 1 and 2 (E-value: 0). We also identified an apolipophorin (E-value: 1.02E-7) (Table S1). The presence of these membrane-associated proteins reinforces the vesicular nature of MSEVs.

Examples of Class 2 proteins include the neural/ectodermal development factor IMP-L2 (E-value: $5.29x10^{-50}$) and a protein involved in pain reception, CG9231 (E-value: $4.39x10^{-15}$). A viral-like Diedel protein (E-value: $1.77x10^{-7}$), viral Enhancin (E-value: $6.02x10^{-5}$), l(2)37Cc (E-value: $3.39x10^{-165}$), odorant binding protein 56d-like (E-value: $5.64x10^{-50}$), major royal jelly protein (E-value: $8.59x10^{-135}$), and two venom acid phosphatases Acph-1 (E-value: $4.12x10^{-5}$) were also found in the Class 2 category; their cDNA sequences were published previously (Heavner et al. 2013) (Table S1). It is possible that these MSEV proteins modulate the hosts' immune responses and/or influence host development to facilitate successful parasitism.

Within Class 3, 45 proteins (90%) lacked BLASTp and InterProScan results. However, Conserved Domain Database (CDD) (Marchler-Bauer et al. 2017) searches returned 9 hits identifying potentially functional domains (Table 1). This included (a) a

CD99L2 like antigen (%ID: 24%, E-value: $3x10^{-3}$), (b) a DEAD-like helicases superfamily member (%ID: 22%, E-value $2x10^{-4}$) and (c) a herpes outer envelope glycoprotein 350 (gp350), (%ID: 28%, E-value: $4x10^{-3}$) (Table 1).

A BLASTp DELTA-BLAST of the potential gp350 domain against the nr database specifying “Vira” (taxid: 10239) under organism resulted in Crimean-Congo hemorrhagic fever orthonairovirus envelope glycoprotein (%ID: 30%, E-value: $2.5x10^{-1}$), Lymphocryptovirus Macaca gp350 (%ID: 29%, E-value: $7.2x10^{-1}$), and Gallid Alphaherpesvirus 1 envelope glycoprotein J (%ID: 26%, E-value: 1.2) as top hits. BLASTp DELTA-BLAST of the potential gp350 domain against the nr database for Hymenoptera yielded an uncharacterized protein as the best hit (%ID: 24%, E-value: $8x10^{-6}$) in the ant *Vollenhovia emeryi*. This ant protein is predicted to contain calcium-binding EGF domains. The second hit in this search is from *N. vitripennis* for a predicted mucin-3A like glycoprotein (Gendler and Spicer 1995) (%ID: 24%, E-value: $2x10^{-4}$). Interestingly, transcripts related to the potential *Lh* gp350-like protein are not found in the *Lb* or *G. hookeri* transcriptomes (Table S1) (Goecks et al. 2013). Presence of this gp350-like protein in *Lh* MSEVs, but its absence in *Lb* MSEVs, suggests that it somehow contributes to differences in *Lh*/*Lb* host-parasite interactions and is therefore worthy of future studies. Complement receptor type 2 (CR2) in human B lymphocytes interacts with gp350 during Epstein-Barr infection (Young et al. 2008) and finding a verified homologue of CR2 in *Drosophila* hosts would be interesting in future research.

Because more than 200 proteins have now been added to the previously described MSEV proteome (Heavner et al. 2017), we re-evaluated our previous enrichment analysis. In an ortholog-based comparison of the superset to human

383 extracellular vesicle (EV) proteomes in Vesiclepedia (the most current and robust
384 source of EV data (Kalra et al. 2012)), we found that the largest proportion of superset
385 proteins (49%) are proteins specifically associated with exosomes (Fig. 1B). In human
386 and mouse EV proteomes, mitochondrial and ribosomal proteins are enriched (Kalra et
387 al. 2012). Accordingly, protein components of mitochondria (e.g., respiratory chain) and
388 ribosomes (e.g., large and small subunit proteins) are found to be highly enriched in the
389 *Lh* MSEV superset. However, we found that the significance of the enrichment was
390 higher between the superset and exosomal proteins than mitochondrial or ribosomal
391 proteins (Fig. 1C). These results demonstrate the similarities in the protein profiles of
392 MSEVs and EVs.
393
394 **Do *Lh* MSEVs contain homologs of PDV or viral proteins?** Even though figitid
395 *Leptopilina* wasps are distantly related to PDV-containing Ichneumonid and Braconid
396 wasps (Misof et al. 2014; Strand and Burke 2015), an association of PDV-like viruses in
397 figitid wasps cannot be discounted because of shared evolutionary history. Recent
398 publications have identified capsid-less VLPs in Ichneumonidae wasps (Volkoff et al.
399 2010; Pichon et al. 2015; Burke et al. 2018) and it is possible that *Lh* MSEVs have a
400 similar viral origin. We therefore analyzed the *Lh* MSEV proteome superset against the
401 GenBank PDV database, and then against its entire Viridae database.
402 To identify false positives, MSEV proteins with positive PDV hits (E-values were
403 less than $1.0x10^{-3}$, %ID was 20% or greater, and query coverage was 30% or higher)
404 were also searched against the unrestricted nr database to compare relatedness. If an
405 MSEV protein is similar to a viral or virus-related PDV protein, we expected that, in the

406 unrestricted nr database search, the MSEV query sequence would align again with the
407 same viral subject sequences, but with a lower E-value (Table S2).
408 For PDV searches (Taxid: 10482 and Taxid: 40273), four proteins returned hits
409 with E-values better than $1.0x10^{-20}$ and query coverage greater than 30%. Three of
410 these hits are conserved proteins (cytochrome P450 and histone 4) while the fourth
411 result identified an uncharacterized *Cotesia congregata* bracovirus (CcBV) protein (%ID:
412 31.08%, E-value: $1.38x10^{-17}$, query coverage: 77%) (Table S2). The unbiased BLASTp
413 search against the entire nr database however had better results against eukaryotic
414 proteins (E values: 0 to $2.0x10^{-7}$ and %ID from 100 to 56.25) (Table S2). In fact, the
415 query that yielded the CcBV protein was better matched to a eukaryotic ribonuclease
416 (%ID: 26.06%, E-value $1.14x10^{-16}$, query coverage: 84%) (Table S2). These results
417 suggest that MSEV sequence similarities with PDV proteins may not be significant.
418 We also searched the *Lh* MSEV superset for presence of *L. boulardi* Filamentous
419 Virus (LbFV) homologs (LbFV is a behavior manipulating virus of *Lb* (Varaldi et al. 2006;
420 Patot et al. 2012)). Of LbFV's 108 genes, 13 are present in genomes of *Lb*, *Lh* and
421 related species, and the 13 transcripts are expressed in the *Lb* venom gland (Di
422 Giovanni et al. 2019). Within our thresholds, we obtained only three (of 13) sequences
423 with similarity to LbFV ORFs. However, these three *Lh* MSEV proteins, with hits for
424 LbFV sequences obtained better scoring hits in the unrestricted nr database, suggesting
425 that the *Lh* MSEV proteins are not highly related to the LbFV proteins (Table S2).
426 When comparing MSEV proteins to the entirety of Viridae, a total of 35 MSEV
427 proteins had hits with %IDs ranging from 30% to 71% and E-values ranging from
428 $1.0x10^{-22}$ to $1.0x10^{-178}$ (Table S2). However, a BLASTp search against the entire nr

database found that proteins with results for viral hits had better scores when searched against the entire nr database, indicating that while viral hits are possible, they are not the best match (Table S2). This result, in addition to the fact that 372 other MSEV proteins (including the Diedel and Enhancin (Table S1)) did not return viral hits, would indicate that a majority of MSEV proteins are not closely related to viral proteins.

The whole-body transcriptome contains expressed MSEV transcripts: We performed a mixed-gender whole-body transcriptome sequencing and *de novo* assembly of *Lh* transcripts. This assembly generated 104,066 transcripts. This dataset is more than three times larger than the published data derived from abdomens of female wasps that has 31,400 transcripts (Goecks et al. 2013). A BLAST analysis of the female abdominal transcripts against the male/female whole-body transcripts showed that a majority (21,493/31,400, 68.44%) were present in the latter data set.

We searched the whole-body transcriptome for MSEV protein coding sequences using tBLASTn. Of 407 MSEV superset proteins, we identified transcripts for 371 (91.15%) proteins. Despite the ~9% discrepancy (likely due to differences in expression levels due to different experimental conditions), these results largely verify the transcript data from (Goecks et al. 2013) that we have based our proteomic analyses on. Of the 371 MSEV transcripts identified, 233 (62.8%) encode Class 1, 44 (11.86%) encode Class 2, and 94/371 (25.34%) encode Class 3 proteins.

Assembly of the *Lh* genome: We separately sequenced *Lh* 14 male and female genomic DNA and assembled the paired-end reads *de novo*, using ABySS (Jackman et

al. 2017). These assemblies have a modest scaffold N50 of 4,800 with more than 100,000 scaffolds and an average coverage of 87% (Table 2). Assembly with MaSurCa (Zimin et al. 2013) provided similar results (data not shown), indicating that our assembly quality is limited likely due to factors such as large genome size and repetitive sequence regions (Dominguez Del Angel et al. 2018). Although the N50 values and large number of scaffolds indicate that the genome is not highly assembled, we found at least 80% of BUSCOs shared in the Insecta set in both assemblies (Table 2, BUSCOs in Table S3).

While still fragmented, a *de novo* joint assembly of male and female sequences using Platanus-allee and AGOUTI improved assembly and scaffolding statistics (N50: 11,906, average coverage 91.1%). The number of found BUSCOs in the joint assembly rose to 90% (Table 2, BUSCOs in Table S3).

Analysis of K-mer multiplicity versus GC content in the genome sequencing reads using the K-mer analysis tool, KAT (Mapleson et al. 2016) showed three possible clusters, although they are difficult to distinguish (Fig. 2A). Cluster 1 has high multiplicity (450-650), Cluster 2 has lower multiplicity and a wide range of GC content, and Cluster 3 has the lowest multiplicity and the highest GC content. Cluster 3 overlaps with Cluster 2 making them hard to fully separate. BLAST searches of a random sample (1,672/4,482) from Cluster 1 contigs hit insect homologs 73% (1,220/1,672) of the time, *Acetobacter* homologs 13% (216/1,672) of the time, and then a variety of mostly Eukaryotic hits. Cluster 2 represents a majority of the wasp genome (>94%), and blast hits of a random sample (316/68,173) of its contigs almost exclusively had homologs in Hymenoptera (311/316; 98%) and mostly in *L. heterotoma* (227/316; 71%). Cluster 3 is

475 the smallest of the three and contigs from Cluster 3 had homologs exclusively in
476 *Acetobacter* (110/110). There was no evidence for contamination from a viral source or
477 discrete MSEV-specific set of nucleic acid sequence.
478 Furthermore, K-mer multiplicity versus GC content for the joint assembly of the
479 *Lh 14* genome (Fig. 2B) showed a very similar heat map to that using the published
480 assembly of *L. clavipes* (Fig. 2C; Bioproject: PRJNA84205 (Kraaijeveld et al. 2016)).
481 The two genomes have a highly similar 27-mer/GC profiles that do not differ statistically
482 (multivariate Cramér test statistic = 114,119, $P = 0.73$, number bootstrap-replicates =
483 1000). The *L. heterotoma* assembly has 27-mers with approximately twice the
484 multiplicity of those found in *L. clavipes*, which may represent increased repeat content
485 in *L. heterotoma* and is supported by an assembly size of over 200 Mb larger than the *L.*
486 *clavipes* genome (463 Mb vs 255 Mb) (Kraaijeveld et al. 2016).
487
488 **MSEV genes are encoded in the wasp genome:** Using our annotation pipeline,
489 28,481 predicted genes were annotated. Within the annotated genes, we found 8 genes
490 for the body color *yellow*, 3 *major royal jelly protein* (*mrjp*) genes, 25 odorant
491 receptor/odorant binding protein coding genes, and 94 gene predictions for *cytochrome*
492 *P450*. Some of these nuclear genes are not only involved in development and cellular
493 processes, but are also included in the MSEV proteome (Table S1 and (Heavner et al.
494 2017)). A search of gene predictions for MSEV proteins via tBLASTn identified 325 of
495 407 (79.85%) MSEV sequences (Table 3). Of these, 153/407 (37.6%) had a percent
496 identity of 95% or greater. Presence or removal of scaffolds with bacterial DNA

sequences from either the separate male/female or the joint assembly did not affect this number, supporting the nuclear location of a majority of the MSEV genes.

As gene prediction software can potentially miss genes (Wang et al. 2004), we searched the genomic scaffolds directly for MSEV-coding sequence regions using known protein sequences as queries via tBLASTn before and after removal of bacterial sequences. In both cases, 375/407 (92.13%) MSEV sequences were at least 70% complete as determined by query coverage (Table 3). Of these, 191/407 (46.9%) had a percent identity of 95% or greater.

The scaffolds containing MSEV genes (Fig. S1A) were also compared to a random subset of scaffolds without MSEV genes (Fig S1B) for their 27-mer/GC profiles. These appeared to not differ statistically (multivariate Cramér test statistic = 3755, P = 0.80, number bootstrap-replicates = 1000), indicating that the MSEV genes lie on scaffolds that resemble the rest of the genome.

Characterization of select MSEV genes: We spot checked small portions of the genome for gene structure predictions of MSEV virulence protein genes *SmGTPse01* (Class 2) and *p40* (Class 3). For this, we sequenced PCR products of gDNA corresponding to these genes.

The MSEV SmGTPase01 has prokaryotic-like GTPase domains and its gene is expected to lack introns (Heavner et al. 2017). The predicted *SmGTPase01* CDS spans 936 bp, which contains the functional GTPase domain (Heavner 2018). Scaffolds from male and female genomes confirmed the absence of coding region introns (data not shown). We hypothesized that primers in 5’ and 3’ untranslated regions (UTRs) should

amplify the exact fragment from cDNA/gDNA as template based on manual characterization of the *SmGTPase01* locus (Heavner 2018) (Fig. 3A). This prediction was borne out and we amplified an 873 bp fragment only from female cDNA and from both male and female gDNA (Fig. 3C). The sequenced PCR products were identical to corresponding sequence within the assembly and the published transcript sequence from Goecks et al. (data not shown).

The *p40* gene encodes a protein that is structurally similar to T3SS bacterial needle tip proteins IpaD/SipD from *Shigella* and *Salmonella*. However, *p40*'s genomic sequence is expected to have introns (Heavner et al. 2017). The full p40 gene was computationally assembled and predicted within both male and female genomes. Primers designed for *p40*'s 5' and 3' UTRs (Goecks et al. 2013; Ramroop 2016) (Fig. 3B), allowed amplification of *p40*'s 939 bp cDNA only in preparations from female wasp extracts, but gDNA bands at 1,630 bp were detected from reactions when either male or female genome was used as template, indicating the presence of introns (Fig. 3D). Sequencing the cloned cDNA product from females confirmed the published cDNA sequence (Heavner et al., 2017). We also cloned and sequenced the gDNA products from male and female wasps and found the sequences to be identical (data not shown).

Unlike the well-characterized *Drosophila* hosts, the biology and molecular-genetics of their parasitic wasps have remained relatively obscure with only recent characterizations of *Leptopilina* and *Ganaspis* spp. (Melk and Govind 1999; Colinet et al. 2013; Goecks et al. 2013; Heavner et al. 2013; Mortimer et al. 2013; Heavner et al. 2017; Di Giovanni et al. 2019; Khan et al. 2018). Our proteomic, transcriptomic and genomic results here expand the available information on *L. heterotoma*. Bioinformatics

analysis of the additional MSEV proteins does not alter the initial interpretation of the original 161 proteomic data. Genomic sequencing and analysis of scaffolds reveals that more than 92% of the MSEV genes reside on the wasp genome. We did not find evidence for MSEV gene association with endosymbiont or commensal bacterial DNA. We suspect that the remaining ~8% are also nuclear genes and this association will be confirmed in higher quality assemblies. Altogether, these results strongly suggest that, like other subcellular structures, MSEVs are encoded in the wasp nuclear genome.

The cellular nature of *Lh* vesicles is likely to be shared by closely related *Lv* and *Lb* wasps. Our previous work has shown that the overall morphologies of *Lh* and *Lv* MSEVs are similar (Morales et al. 2005; Chiu et al. 2006). However, this is not the case for *Lb* MSEVs; different *Lb* strains have varying MSEV morphologies (Dupas et al. 1996; Gueguen et al. 2011; Wan et al. 2019). Interpretation of their identity also varies. For example, Di Giovanni et al. (Di Giovanni et al. 2019) contend that MSEVs/VLPs are derived from a virus ancestral to the LbFV. Our analysis of the expanded proteomic superset does not lend strong support to this line of thinking.

We did not find convincing evidence of PDV or other viral structural proteins in the *Lh* MSEV proteome. However, we cannot discount that MSEVs have a viral origin as our analysis is limited by the fragmentation of the genome. It is also possible that a virus related to MSEVs may not have been identified to date. Mechanistically, eukaryotic viruses and vesicles share cellular pathways involving the endomembrane systems of their cells of origin or their target cells (Nolte-‘t Hoen et al. 2016), leading to overlap in protein functionality, but not necessarily origin. Thus, at least some of the Class 1 proteins in the MSEV proteome may be central to MSEV biogenesis in the wasp

or for their interactions with the host hemocytes' endomembrane machinery despite potentially being related to viruses. It is noteworthy that energy metabolism genes appear to be involved in rapid speciation and adaptation to new environments (Gershoni et al. 2009; Lane 2009), raising the possibility that MSEV mitochondrial proteins might contribute to this process. How *Lh* MSEVs are functionally similar to other insect or mammalian EVs remains to be explored experimentally. Functional characterization of predicted infection and immunity Class 2 proteins should explain the immune-suppressive strategies of these wasps. RNA interference, infection assays, and other experimental strategies should make this line of inquiry feasible.

Functional assignments are difficult for the unannotated Class 3 proteins. These are likely to be quite interesting, due to their different expression profiles in *Lh* versus *Lb* and *G. hookeri* species. This difference in expression may stem either from *cis* changes in their regulatory sequences, or from absence of these genes in the *Lb* or *G. hookeri* genomes. Recent comparative genomics analysis has shown that over 40% of venom genes in the closely-related species *N. vitripennis* and *N. giraulti* have diverged significantly and up to 25% of venom genes are specific to a species (Martinson et al. 2017). A proteomic analysis of the venom genes of *Leptopilina spp*. and a molecular understanding of their expression will provide insights into how key activities within MSEVs evolved to parasitize the range of fruit fly hosts.

A key question regarding *Lh* virulence proteins critical to wasp success is whether their genes reside in a discrete region of the genome like a "virulence island" found in some microbial genomes (Dobrindt et al. 2004; Gal-Mor and Finlay 2006), or whether some genes are dispersed within the genome, while others occur in one or

589 more clusters as in wasps with PDVs (Volkoff et al. 2010; Pichon et al. 2015). More
590 complete assemblies, scaffolded to the level of chromosomes, will describe the
591 genome-wide distribution of these genes in *Lh* and related wasps. Key MSEV genes
592 could serve as genetic markers in future studies. Comparative genomics will uncover
593 additional gene family members of MSEV proteins in other *Leptopilina* wasps and
594 enable the development of new functional genomics tools such as CRISPR-disrupted
595 mutant alleles made in *N. vitripennis* (Werren et al. 2009; Siebert et al. 2015; Li et al.
596 2017b; Li et al. 2017a). These approaches will open new avenues for understanding the
597 biology of this host-parasite model.

598

ACKNOWLEDGEMENTS

We thank Drs. W. Qiu and S. Singh, and J. Chou for discussions and critical comments, and our reviewers for insightful feedback. We are grateful to A. Corvelo at the New York Genome Center for help with genome assemblies. Bioinformatics work was conducted in-house and with the BIOMIX Shared Computing Cluster at Delaware Biotechnology Institute, University of Delaware. This work was supported by grants from NASA (NNX15AB42G), NSF (IOS-1121817), NIH (1F31GM111052-01A1, 5G12MD007603-30, and GM103446).

LITERATURE CITED

Almagro Armenteros, J.J., K.D. Tsirigos, C.K. Sonderby, T.N. Petersen, O. Winther *et al.*, 2019 SignalP 5.0 improves signal peptide predictions using deep neural networks. *Nat Biotechnol* 37 (4):420-423.

Altschul, S.F., W. Gish, W. Miller, E.W. Myers, and D.J. Lipman, 1990 Basic local alignment search tool. *J Mol Biol* 215 (3):403-410.

Ashburner, M., C.A. Ball, J.A. Blake, D. Botstein, H. Butler *et al.*, 2000 Gene ontology: tool for the unification of biology. The Gene Ontology Consortium. *Nat Genet* 25 (1):25-29.

Baringhaus, L., and C. Franz, 2004 On a new multivariate two-sample test. 88 (1):190-206.

Buchfink, B., C. Xie, and D.H. Huson, 2015 Fast and sensitive protein alignment using DIAMOND. *Nature Methods* 12 (1):59-60.

Burke, G.R., T.J. Simmonds, B.J. Sharanowski, and S.M. Geib, 2018 Rapid Viral Symbiogenesis via Changes in Parasitoid Wasp Genome Architecture. *Mol Biol Evol* 35 (10):2463-2474.

Camacho, C., G. Coulouris, V. Avagyan, N. Ma, J. Papadopoulos *et al.*, 2009 BLAST+: architecture and applications. *BMC Bioinformatics* 10:421.

Carbon, S., E. Douglass, N. Dunn, B. Good, N.L. Harris *et al.*, 2019 The Gene Ontology Resource: 20 years and still GOing strong. *Nucleic Acids Research* 47 (D1):D330-D338.

629 Chiu, H., and S. Govind, 2002 Natural infection of D. melanogaster by virulent parasitic
630 wasps induces apoptotic depletion of hematopoietic precursors. *Cell Death Differ*
631 9 (12):1379-1381.
632 Chiu, H., J. Morales, and S. Govind, 2006 Identification and immuno-electron
633 microscopy localization of p40, a protein component of immunosuppressive
634 virus-like particles from Leptopilina heterotoma, a virulent parasitoid wasp of
635 Drosophila. *J Gen Virol* 87 (Pt 2):461-470.
636 Cock, P.J.A., T. Antao, J.T. Chang, B.A. Chapman, C.J. Cox *et al.*, 2009 Biopython:
637 freely available Python tools for computational molecular biology and
638 bioinformatics. *Bioinformatics* 25 (11):1422-1423.
639 Colinet, D., E. Deleury, C. Anselme, D. Cazes, J. Poulain *et al.*, 2013 Extensive inter-
640 and intraspecific venom variation in closely related parasites targeting the same
641 host: the case of Leptopilina parasitoids of Drosophila. *Insect Biochem Mol Biol*
642 43 (7):601-611.
643 Conesa, A., S. Götz, J.M. García-Gómez, J. Terol, M. Talón *et al.*, 2005 Blast2GO: a
644 universal tool for annotation, visualization and analysis in functional genomics
645 research. *Bioinformatics* 21 (18):3674-3676.
646 Consortium, U., 2015 UniProt: a hub for protein information. *Nucleic Acids Res* 43
647 (Database issue):D204-212.
648 Crotti, E., A. Rizzi, B. Chouaia, I. Ricci, G. Favia *et al.*, 2010 Acetic Acid Bacteria, Newly
649 Emerging Symbionts of Insects. *Applied and Environmental Microbiology* 76
650 (21):6963-6970.

651 Di Giovanni, D., D. Lepetit, M. Boulesteix, Y. Couté, M. Ravallec *et al.*, 2019 A behavior-
652 manipulating virus relative as a source of adaptive genes for parasitoid wasps.
653 *bioRxiv*:342758.
654 Dobrindt, U., B. Hochhut, U. Hentschel, and J. Hacker, 2004 Genomic islands in
655 pathogenic and environmental microorganisms. *Nat Rev Microbiol* 2 (5):414-424.
656 Dominguez Del Angel, V., E. Hjerde, L. Sterck, S. Capella-Gutierrez, C. Notredame *et*
657 *al.*, 2018 Ten steps to get started in Genome Assembly and Annotation.
658 *F1000Res* 7.
659 Drezen, J.M., M. Leobold, A. Bezier, E. Huguet, A.N. Volkoff *et al.*, 2017 Endogenous
660 viruses of parasitic wasps: variations on a common theme. *Curr Opin Virol* 25:41-
661 48.
662 Dupas, S., M. Brehelin, F. Frey, and Y. Carton, 1996 Immune suppressive virus-like
663 particles in a Drosophila parasitoid: significance of their intraspecific
664 morphological variations. *Parasitology* 113 (Pt 3):207-212.
665 Engel, P., and N.A. Moran, 2013 The gut microbiota of insects - diversity in structure
666 and function. *Fems Microbiology Reviews* 37 (5):699-735.
667 Franz, C., 2019 cramer: Multivariate Nonparametric Cramer-Test for the Two-Sample-
668 Problem. R package version 0.9-3. https://CRAN.R-project.org/package=cramer.
669 Gal-Mor, O., and B.B. Finlay, 2006 Pathogenicity islands: a molecular toolbox for
670 bacterial virulence. *Cell Microbiol* 8 (11):1707-1719.
671 Gauthier, J., J.M. Drezen, and E.A. Herniou, 2018 The recurrent domestication of
672 viruses: major evolutionary transitions in parasitic wasps. *Parasitology* 145
673 (6):713-723.

674 Gendler, S.J., and A.P. Spicer, 1995 Epithelial mucin genes. *Annu Rev Physiol* 57:607-
675 634.
676 Gershoni, M., A.R. Templeton, and D. Mishmar, 2009 Mitochondrial bioenergetics as a
677 major motive force of speciation. *Bioessays* 31 (6):642-650.
678 Goecks, J., N.T. Mortimer, J.A. Mobley, G.J. Bowersock, J. Taylor *et al.*, 2013
679 Integrative approach reveals composition of endoparasitoid wasp venoms. *PLoS*
680 *One* 8 (5):e64125.
681 Grabherr, M.G., B.J. Haas, M. Yassour, J.Z. Levin, D.A. Thompson *et al.*, 2011 Full-
682 length transcriptome assembly from RNA-Seq data without a reference genome.
683 *Nature Biotechnology* 29 (7):644-U130.
684 Gueguen, G., B. Onemola, and S. Govind, 2012 Association of a new Wolbachia strain
685 with, and its effects on, Leptopilina victoriae, a virulent wasp parasitic to
686 Drosophila spp. *Appl Environ Microbiol* 78 (16):5962-5966.
687 Gueguen, G., R. Rajwani, I. Paddibhatla, J. Morales, and S. Govind, 2011 VLPs of
688 Leptopilina boulardi share biogenesis and overall stellate morphology with VLPs
689 of the heterotoma clade. *Virus Res* 160 (1-2):159-165.
690 Götz, S., J.M. García-Gómez, J. Terol, T.D. Williams, S.H. Nagaraj *et al.*, 2008 High-
691 throughput functional annotation and data mining with the Blast2GO suite.
692 *Nucleic Acids Res* 36 (10):3420-3435.
693 Heavner, M.E., 2018 Evidence for Organelle-like Extracellular Vesicles From a Parasite
694 of Drosophila and Their Function in Suppressing Host Immunity, pp. 236 in
695 *Biochemistry*. City University of New York, Graduate Center.

Heavner, M.E., G. Gueguen, R. Rajwani, P.E. Pagan, C. Small *et al.*, 2013 Partial venom gland transcriptome of a Drosophila parasitoid wasp, Leptopilina heterotoma, reveals novel and shared bioactive profiles with stinging Hymenoptera. *Gene* 526 (2):195-204.

Heavner, M.E., A.D. Hudgins, R. Rajwani, J. Morales, and S. Govind, 2014 Harnessing the natural D*rosophila*-parasitoid model for integrating insect immunity with functional venomics. *Curr Opin Insect Sci* 6:61-67.

Heavner, M.E., J. Ramroop, G. Gueguen, G. Ramrattan, G. Dolios *et al.*, 2017 Novel Organelles with Elements of Bacterial and Eukaryotic Secretion Systems Weaponize Parasites of Drosophila. *Curr Biol* 27 (18):2869-2877.e2866.

Ihaka, R., and R. Gentleman, 1996 R: A Language for Data Analysis and Graphics. *Journal of Computational and Graphical Statistics* 5 (3):299-314.

Jackman, S.D., B.P. Vandervalk, H. Mohamadi, J. Chu, S. Yeo *et al.*, 2017 ABySS 2.0: resource-efficient assembly of large genomes using a Bloom filter. *Genome Res* 27 (5):768-777.

Johnson, M., I. Zaretskaya, Y. Raytselis, Y. Merezhuk, S. McGinnis *et al.*, 2008 NCBI BLAST: a better web interface. *Nucleic Acids Res* 36 (Web Server issue):W5-9.

Jones, P., D. Binns, H.Y. Chang, M. Fraser, W. Li *et al.*, 2014 InterProScan 5: genome-scale protein function classification. *Bioinformatics* 30 (9):1236-1240.

Kajitani, R., D. Yoshimura, M. Okuno, Y. Minakuchi, H. Kagoshima *et al.*, 2019 Platanus-allee is a de novo haplotype assembler enabling a comprehensive access to divergent heterozygous regions. *Nature Communications* 10.

718 Kall, L., A. Krogh, and E.L. Sonnhammer, 2004 A combined transmembrane topology
719 and signal peptide prediction method. *J Mol Biol* 338 (5):1027-1036.
720 Kall, L., A. Krogh, and E.L.L. Sonnhammer, 2007 Advantages of combined
721 transmembrane topology and signal peptide prediction - the Phobius web server.
722 *Nucleic Acids Research* 35:W429-W432.
723 Kalra, H., R.J. Simpson, H. Ji, E. Aikawa, P. Altevogt *et al.*, 2012 Vesiclepedia: a
724 compendium for extracellular vesicles with continuous community annotation.
725 *PLoS Biol* 10 (12):e1001450.
726 Kanehisa, M., Y. Sato, and K. Morishima, 2016 BlastKOALA and GhostKOALA: KEGG
727 Tools for Functional Characterization of Genome and Metagenome Sequences. *J*
728 *Mol Biol* 428 (4):726-731.
729 Keebaugh, E.S., and T.A. Schlenke, 2014 Insights from natural host-parasite
730 interactions: The Drosophila model. *Developmental and Comparative*
731 *Immunology* 42 (1):111-123.
732 Keller, O., M. Kollmar, M. Stanke, and S. Waack, 2011 A novel hybrid gene prediction
733 method employing protein multiple sequence alignments. *Bioinformatics* 27
734 (6):757-763.
735 Khan, S., D.T. Sowpati, and R.K. Mishra, 2018 Long-read genome sequence and
736 assembly of Leptopilina boulardi: a specialist Drosophila parasitoid. *bioRxiv*.
737 Kim, D., B. Landmead, and S.L. Salzberg, 2015 HISAT: a fast spliced aligner with low
738 memory requirements. *Nature Methods* 12 (4):357-U121.

739 Kraaijeveld, K., S.Y. Anvar, J. Frank, A. Schmitz, J. Bast *et al.*, 2016 Decay of Sexual
740 Trait Genes in an Asexual Parasitoid Wasp. *Genome Biology and Evolution* 8
741 (12):3685-3695.
742 Krogh, A., B. Larsson, G. von Heijne, and E.L. Sonnhammer, 2001 Predicting
743 transmembrane protein topology with a hidden Markov model: application to
744 complete genomes. *J Mol Biol* 305 (3):567-580.
745 Labrosse, C., K. Staslak, J. Lesobre, A. Grangeia, E. Huguet *et al.*, 2005 A RhoGAP
746 protein as a main immune suppressive factor in the Leptopilina boulardi
747 (Hymenoptera, Figitidae) - Drosophila melanogaster interaction. *Insect*
748 *Biochemistry and Molecular Biology* 35 (2):93-103.
749 Lane, N., 2009 On the origin of bar codes. *Nature* 462 (7271):272-274.
750 Li, H., and R. Durbin, 2009 Fast and accurate short read alignment with Burrows-
751 Wheeler transform. *Bioinformatics* 25 (14):1754-1760.
752 Li, M., L.Y.C. Au, D. Douglah, A. Chong, B.J. White *et al.*, 2017a Generation of heritable
753 germline mutations in the jewel wasp Nasonia vitripennis using CRISPR/Cas9.
754 *Sci Rep* 7 (1):901.
755 Li, M., M. Bui, and O.S. Akbari, 2017b Embryo Microinjection and Transplantation
756 Technique for Nasonia vitripennis Genome Manipulation. *J Vis Exp* (130).
757 Li, W., A. Cowley, M. Uludag, T. Gur, H. McWilliam *et al.*, 2015 The EMBL-EBI
758 bioinformatics web and programmatic tools framework. *Nucleic Acids Res* 43
759 (W1):W580-584.

760 Mapleson, D., G. Garcia Accinelli, G. Kettleborough, J. Wright, and B.J. Clavijo, 2016
761 KAT: a K-mer analysis toolkit to quality control NGS datasets and genome
762 assemblies. *Bioinformatics* 33 (4):574-576.
763 Marchler-Bauer, A., Y. Bo, L. Han, J. He, C.J. Lanczycki *et al.*, 2017 CDD/SPARCLE:
764 functional classification of proteins via subfamily domain architectures. *Nucleic*
765 *Acids Res* 45 (D1):D200-D203.
766 Martinson, E.O., Mrinalini, Y.D. Kelkar, C.H. Chang, and J.H. Werren, 2017 The
767 Evolution of Venom by Co-option of Single-Copy Genes. *Curr Biol* 27 (13):2007-
768 2013.e2008.
769 Melk, J.P., and S. Govind, 1999 Developmental analysis of Ganaspis xanthopoda, a
770 larval parasitoid of Drosophila melanogaster. *J Exp Biol* 202 (Pt 14):1885-1896.
771 Mikheenko, A., G. Valin, A. Prjibelski, V. Saveliev, and A. Gurevich, 2016 Icarus:
772 visualizer for de novo assembly evaluation. *Bioinformatics* 32 (21):3321-3323.
773 Misof, B., S. Liu, K. Meusemann, R.S. Peters, A. Donath *et al.*, 2014 Phylogenomics
774 resolves the timing and pattern of insect evolution. *Science* 346 (6210):763-767.
775 Morales, J., H. Chiu, T. Oo, R. Plaza, S. Hoskins *et al.*, 2005 Biogenesis, structure, and
776 immune-suppressive effects of virus-like particles of a Drosophila parasitoid,
777 Leptopilina victoriae. *J Insect Physiol* 51 (2):181-195.
778 Mortimer, N.T., J. Goecks, B.Z. Kacsoh, J.A. Mobley, G.J. Bowersock *et al.*, 2013
779 Parasitoid wasp venom SERCA regulates Drosophila calcium levels and inhibits
780 cellular immunity. *Proc Natl Acad Sci U S A* 110 (23):9427-9432.
781 Narendran, T.C., 2001 Parasitic Hymenoptera and Biological Control, pp. 1-12 in
782 *Biocontrol Potential and its Exploitation in Sustainable Agriculture: Volume 2:*

Insect Pests, edited by R.K. Upadhyay, K.G. Mukerji and B.P. Chamola. Springer US, Boston, MA.

Nielsen, H., 2017 Predicting Secretory Proteins with SignalP. *Methods Mol Biol* 1611:59-73.

Nolte-'t Hoen, E., T. Cremer, R.C. Gallo, and L.B. Margolis, 2016 Extracellular vesicles and viruses: Are they close relatives? *Proceedings of the National Academy of Sciences* 113 (33):9155-9161.

Pannebakker, B.A., L.P. Pijnacker, B.J. Zwaan, and L.W. Beukeboom, 2004 Cytology of Wolbachia-induced parthenogenesis in Leptopilina clavipes (Hymenoptera: Figitidae). *Genome* 47 (2):299-303.

Pathan, M., P. Fonseka, S.V. Chitti, T. Kang, R. Sanwlani *et al.*, 2019 Vesiclepedia 2019: a compendium of RNA, proteins, lipids and metabolites in extracellular vesicles. *Nucleic Acids Res* 47 (D1):D516-D519.

Pathan, M., S. Keerthikumar, C.S. Ang, L. Gangoda, C.Y. Quek *et al.*, 2015 FunRich: An open access standalone functional enrichment and interaction network analysis tool. *Proteomics* 15 (15):2597-2601.

Pathan, M., S. Keerthikumar, D. Chisanga, R. Alessandro, C.S. Ang *et al.*, 2017 A novel community driven software for functional enrichment analysis of extracellular vesicles data. *J Extracell Vesicles* 6 (1):1321455.

Patot, S., R. Allemand, F. Fleury, and J. Varaldi, 2012 An inherited virus influences the coexistence of parasitoid species through behaviour manipulation. *Ecol Lett* 15 (6):603-610.

Pichon, A., A. Bézier, S. Urbach, J.M. Aury, V. Jouan *et al.*, 2015 Recurrent DNA virus domestication leading to different parasite virulence strategies. *Sci Adv* 1 (10):e1501150.

Pritchard, L., J.A. White, P.R.J. Birch, and I.K. Toth, 2006 GenomeDiagram: a python package for the visualization of large-scale genomic data. *Bioinformatics* 22 (5):616-617.

Ramroop, J., 2016 Mechanisms of Immune Activation and Suppression by Parasitic Wasps of Drosophila in *Biology*. Graduate Center, City University of New York.

Rizki, T.M., R.M. Rizki, and Y. Carton, 1990 Leptopilina heterotoma and L. boulardi: strategies to avoid cellular defense responses of Drosophila melanogaster. *Exp Parasitol* 70 (4):466-475.

Rodriguez, J.J., J.L. Fernandez-Triana, M.A. Smith, D.H. Janzen, W. Hallwachs *et al.*, 2013 Extrapolations from field studies and known faunas converge on dramatically increased estimates of global microgastrine parasitoid wasp species richness (Hymenoptera: Braconidae). *Insect Conservation and Diversity* 6 (4):530-536.

Schlenke, T.A., J. Morales, S. Govind, and A.G. Clark, 2007 Contrasting infection strategies in generalist and specialist wasp parasitoids of Drosophila melanogaster. *PLoS Pathog* 3 (10):1486-1501.

Siebert, A.L., D. Wheeler, and J.H. Werren, 2015 A new approach for investigating venom function applied to venom calreticulin in a parasitoid wasp. *Toxicon*.

826 Simão, F.A., R.M. Waterhouse, P. Ioannidis, E.V. Kriventseva, and E.M. Zdobnov, 2015
827 BUSCO: assessing genome assembly and annotation completeness with single-
828 copy orthologs. *Bioinformatics* 31 (19):3210-3212.
829 Small, C., I. Paddibhatla, R. Rajwani, and S. Govind, 2012 An introduction to parasitic
830 wasps of Drosophila and the antiparasite immune response. *J Vis Exp*
831 (63):e3347.
832 Smith-Unna, R., C. Boursnell, R. Patro, J.M. Hibberd, and S. Kelly, 2016 TransRate:
833 reference-free quality assessment of de novo transcriptome assemblies.
834 *Genome Research* 26 (8):1134-1144.
835 Sonnhammer, E.L., G. von Heijne, and A. Krogh, 1998 A hidden Markov model for
836 predicting transmembrane helices in protein sequences. *Proc Int Conf Intell Syst*
837 *Mol Biol* 6:175-182.
838 Stanke, M., and B. Morgenstern, 2005 AUGUSTUS: a web server for gene prediction in
839 eukaryotes that allows user-defined constraints. *Nucleic Acids Res* 33 (Web
840 Server issue):W465-467.
841 Stanke, M., R. Steinkamp, S. Waack, and B. Morgenstern, 2004 AUGUSTUS: a web
842 server for gene finding in eukaryotes. *Nucleic Acids Res* 32 (Web Server
843 issue):W309-312.
844 Strand, M.R., and G.R. Burke, 2015 Polydnaviruses: From discovery to current insights.
845 *Virology* 479-480:393-402.
846 Trapnell, C., A. Roberts, L. Goff, G. Pertea, D. Kim *et al.*, 2012 Differential gene and
847 transcript expression analysis of RNA-seq experiments with TopHat and
848 Cufflinks. *Nat Protoc* 7 (3):562-578.

Varaldi, J., S. Petit, M. Boulétreau, and F. Fleury, 2006 The virus infecting the parasitoid Leptopilina boulardi exerts a specific action on superparasitism behaviour. *Parasitology* 132 (Pt 6):747-756.

Volkoff, A.N., V. Jouan, S. Urbach, S. Samain, M. Bergoin *et al.*, 2010 Analysis of virion structural components reveals vestiges of the ancestral ichnovirus genome. *PLoS Pathog* 6 (5):e1000923.

Wan, B., E. Goguet, M. Ravallec, O. Pierre, S. Lemauf *et al.*, 2019 Venom Atypical Extracellular Vesicles as Interspecies Vehicles of Virulence Factors Involved in Host Specificity: The Case of a Drosophila Parasitoid Wasp. *Frontiers in Immunology* 10 (1688).

Wang, Z., Y. Chen, and Y. Li, 2004 A brief review of computational gene prediction methods. *Genomics Proteomics Bioinformatics* 2 (4):216-221.

Waterhouse, R.M., M. Seppey, F.A. Simão, M. Manni, P. Ioannidis *et al.*, 2017 BUSCO applications from quality assessments to gene prediction and phylogenomics. *Mol Biol Evol*.

Werren, J.H., L. Baldo, and M.E. Clark, 2008 Wolbachia: master manipulators of invertebrate biology. *Nat Rev Microbiol* 6 (10):741-751.

Werren, J.H., D.W. Loehlin, and J.D. Giebel, 2009 Larval RNAi in Nasonia (parasitoid wasp). *Cold Spring Harb Protoc* 2009 (10):pdb.prot5311.

Young, K.A., A.P. Herbert, P.N. Barlow, V.M. Holers, and J.P. Hannan, 2008 Molecular basis of the interaction between complement receptor type 2 (CR2/CD21) and Epstein-Barr virus glycoprotein gp350. *J Virol* 82 (22):11217-11227.

Zhang, S.V., L.T. Zhuo, and M.W. Hahn, 2016 AGOUTI: improving genome assembly and annotation using transcriptome data. *Gigascience* 5.

Zimin, A.V., G. Marcais, D. Puiu, M. Roberts, S.L. Salzberg *et al.*, 2013 The MaSuRCA genome assembler. *Bioinformatics* 29 (21):2669-2677.

877

FIGURES

A.

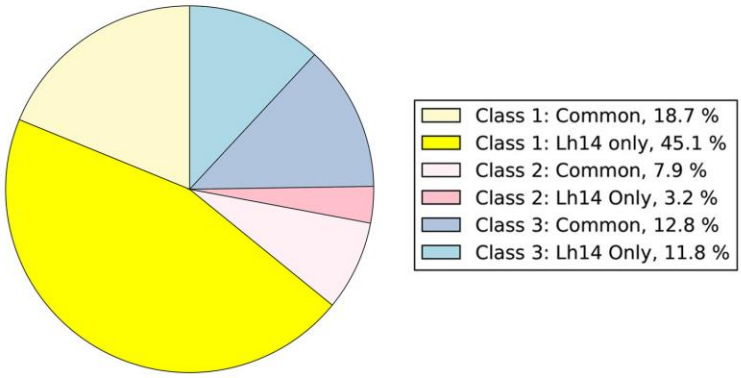

B.

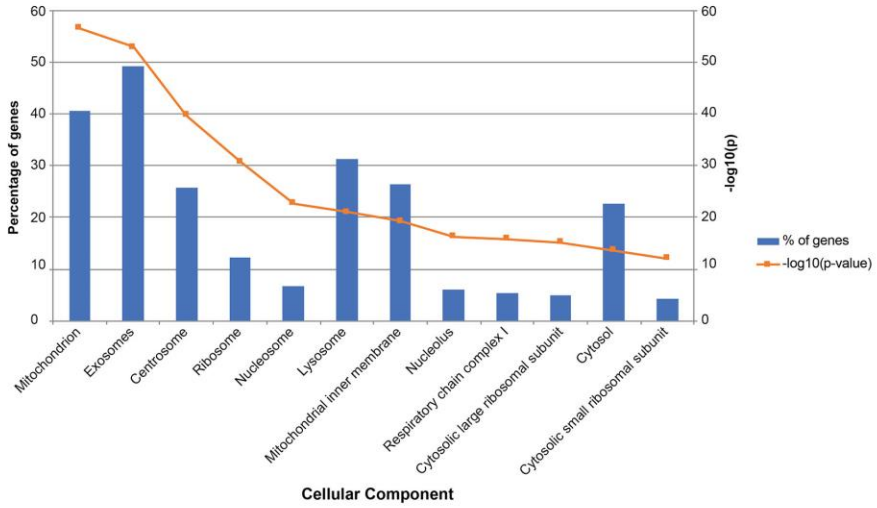

C.

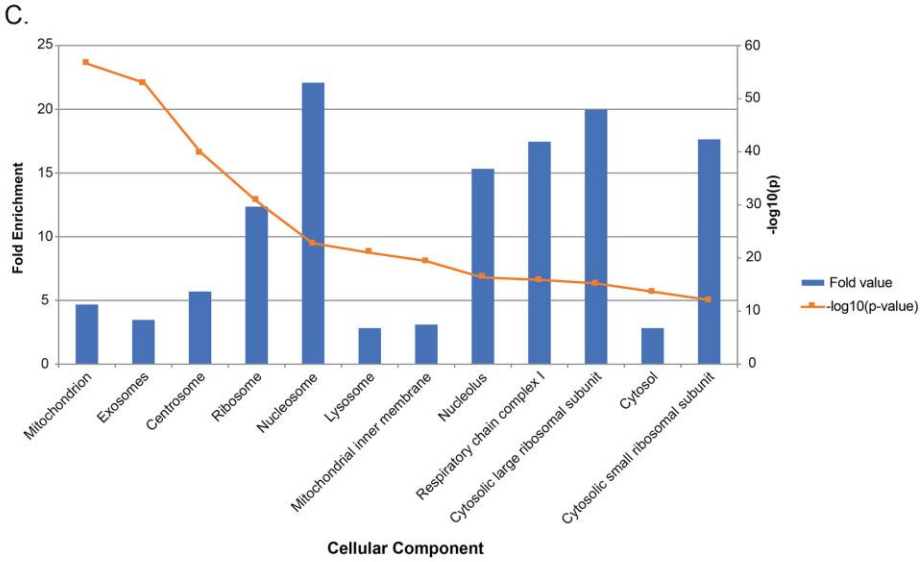

878

Figure 1. The superset of MSEV proteins: (A) *Lh* 14 MSEV proteins were annotated using BLAST2GO prior to class sorting via annotation and GO Terms. Wedges denoted as "Common," were previously published in (Heavner et al. 2017) and represent proteins found in both *Lh* 14 and *Lh* NY MSEV proteomes. New proteins analyzed in this work are in wedges labeled "*Lh* 14 Only." A majority of proteins belong to Class 1. Table S1 lists 246 proteins added to the superset *Lh* 14 proteome. (B) and (C) Enrichment analysis of MSEV superset shows high association with exosomes and mitochondria compared to other cellular organelles according to Vesiclepedia. $-\log_{10}$ (p-value) trend shown in orange for both graphs. The p-values were calculated with the Bonferroni method. (B) Percentage of MSEV genes associated with specific cellular compartments found in Vesiclepedia, relative to all MSEV genes. Of the superset proteins, 41 and 49% are associated with mitochondria and exosomes, respectively ($p = 3 \times 10^{-57}$; 1×10^{-53}). (C) Fold-enrichment of the MSEV dataset in specific cellular compartments. Although many protein classes are present in the proteome, exosomal and mitochondrial proteins show more significant enrichments.

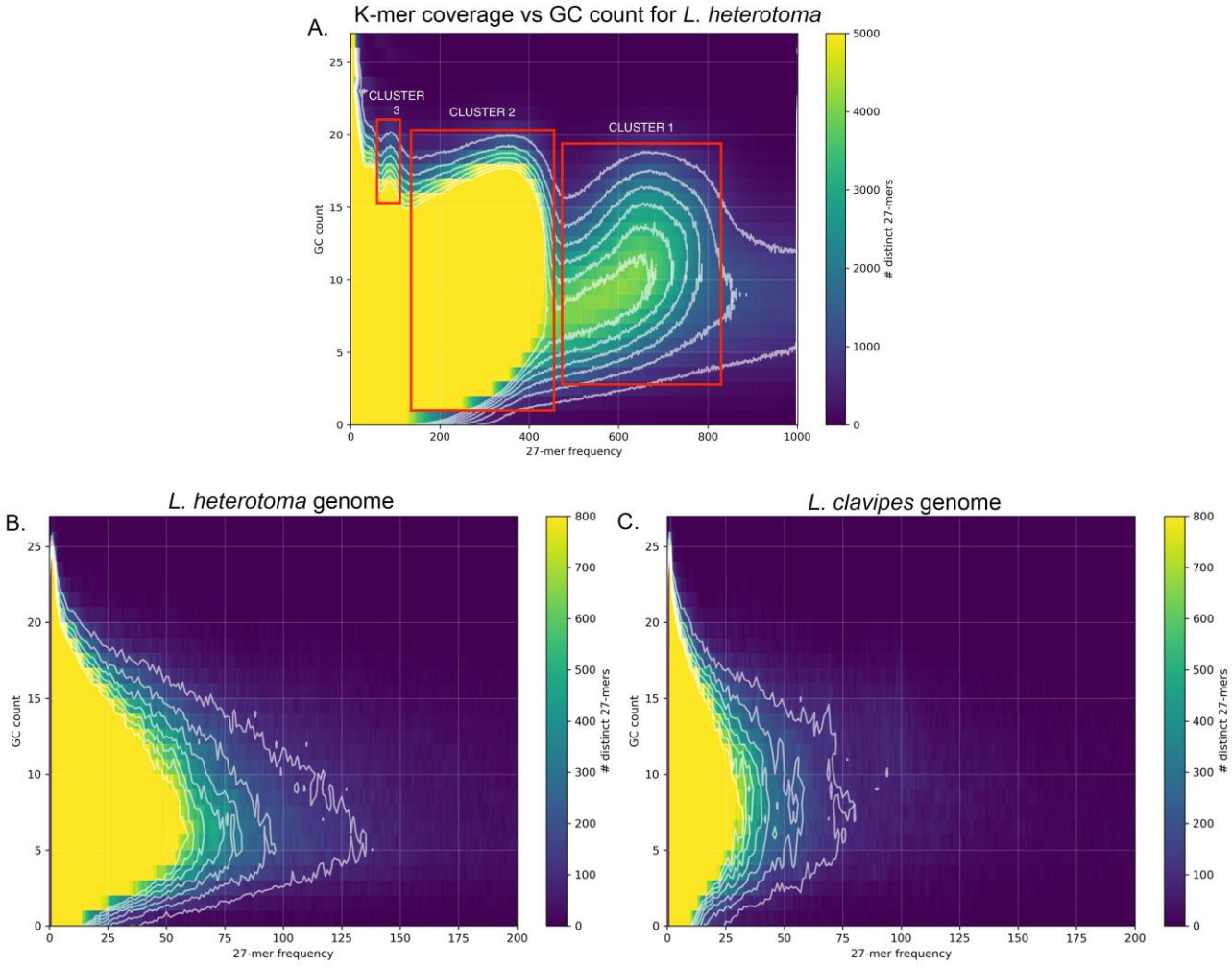

Figure 2. Analysis of K-mer coverage versus GC count. (A) Analysis of genomic reads. 27-mers generated from the cleaned Illumina reads used to assemble the *L. heterotoma* genome binned by their GC count vs multiplicity (total counts among the reads). Bins are colored by the number of distinct K-mers. Different clusters are identified as shown and described in the text. (B and C): A map of 27-mer multiplicity versus GC content of the joint assembly of the *Lh 14* genome (B) to a map from the published *L. clavipes* genome (Bioproject: PRJNA84205) (C).

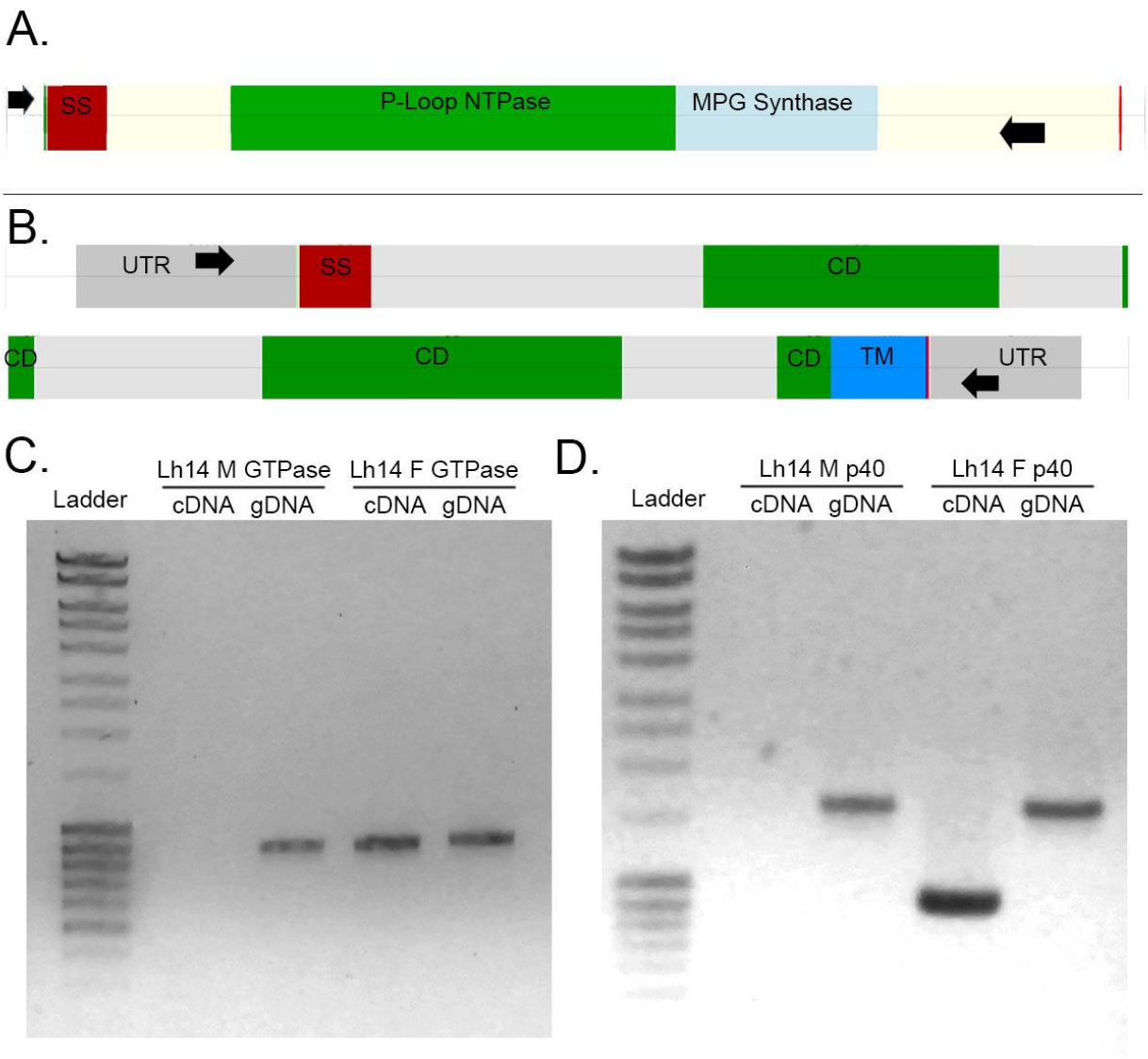

904

905 Figure 3. Predicted gene structures verified by PCR amplification experiments (A, B).
906 Diagrams showing primer locations and predicted gene structures of *SmGTPase01* (A)
907 and *p40* (B). Black arrows indicate primer locations, light gray indicates introns, UTR
908 regions are dark gray and labeled, exons encoding potential protein domains are
909 labeled as shown. Cream colored regions in panel A do not have a specified domain.
910 Diagrams were drawn using GenomeDiagram as part of the Biopython (v. 1.6) package
911 (Pritchard et al. 2006; Cock et al. 2009). Each row in the panels A and B diagrams

corresponds to approximately 1,000 bp. For primer sequences, see methods. (C and D) Ladder is Thermo Fisher MassRuler ladder. (C) PCR products for *SmGTPase01* from male or female cDNA and gDNA. All products are 873 bp long. Male cDNA PCR was negative. (D) PCR products for *p40* from male or female cDNA and gDNA. The expected band for *p40* cDNA is 939 bp and for gDNA is 1,630 bp. Male cDNA PCR was negative. Sequence analysis of PCR amplification products confirmed gene prediction results.

TABLES

MSEV SUPERSET UNKNOWNS CDD-SEARCH RESULTS						
Query (in-house ID)	PSSM-ID	From	To	E-Value	Accession	Short name
GAJC01013214.1_14	**331760**	**25**	**98**	**0.000176**	cl26939	DEXDc superfamily
GAJC01012558.1_12	**330317**	**39**	**205**	**0.003987**	cl25496	Herpes_BLLF1 superfamily/gp350
GAJC01011863.1_13	**311912**	**86**	**187**	**0.003653**	cl07006	RNA_polI_A34 superfamily
GAJC01011463.1_48	**315064**	**234**	**335**	**0.002964**	cl13702	CD99L2 superfamily
GAJC01010930.1_16	**328726**	**32**	**61**	**0.001252**	cl21457	ICL_KPHMT superfamily
GAJC01010353.1_14	**331876**	**31**	**121**	**0.001483**	cl27055	MutS_III superfamily
GAJC01009713.1_25	**311628**	**138**	**225**	**0.000133**	cl06688	TSGP1 superfamily
GAJC01009493.1_4	**328724**	**79**	**96**	**0.001983**	cl21455	P-loop_NTPase superfamily
GAJC01002124.1_43	**330572**	**4**	**269**	**0.0073146**	cl25751	DUF4045 superfamily

Table 1. CDD-search results of MSEV “un-annotated” proteins in the super-set. MSEV ORFs that completed the BLAST2GO pipeline and did not return any results were run through the NCBI CDD-Search Version 3.16 (Accessed: Aug. 2018). Of 45 queries, only 9 returned hits with threshold set to $1x10^{-2}$. The ninth result came from a search with E-value threshold set to 1. Results listed are all unique, high scoring hits for each ORF that returned hits from the search.

ASSEMBLY STATISTICS				
		Male	Female	Joint
Assembly	N50 (bp)	**4,779**	**4,843**	**11906**
	No. scaffolds	**147,558**	**147,549**	**83,487**
	Largest scaffold (bp)	**306,667**	**176,371**	**375,275**
	Total length (bp)	**474,383,205**	**472,302,230**	**462,564,754**
	GC%	**27.54**	**27.28**	**27.84**
	Coverage (%)	**87.7**	**86.8**	**91.1**
BUSCOs (Insecta)	Complete	**80.20%**	**81.30%**	**90.90%**
	Single	**69.40%**	**71.80%**	**89.20%**
	Duplicated	**10.80%**	**9.50%**	**1.70%**
	Fragmented	**15.90%**	**15.10%**	**6.50%**
	Missing	**3.90%**	**3.60%**	**2.60%**
	n	**1658**	**1658**	**1658**

Table 2. Assembly statistics: Statistics of male, female, and combined (male plus female) *Lh* genomes as assessed by QUASTv4.0 and BUSCOv9.0. Percent coverage was found by mapping sequencing reads back to assembly using HISAT2. The identified BUSCOs can be found in Table S1. The QUAST program was run with parameters set for eukaryotic genomes and scaffolds. The BUSCO program was run with species set to 'Nasonia.' Contigs smaller than 500 bp were excluded.

MSEV GENES FOUND IN GENOME ANALYSIS				
	MSEV BLASTn scaffold results		AUGUSTUS prediction results	
	Found	Percentage	Found	Percentage
Female	**278**	**68.3**	**169**	**41.52**
Male	**275**	**67.58**	**166**	**40.78**
Shared in M+F	**265**		**159**	
Joint Assembly	**375**	**92.13%**	**325**	**79.85%**

Table 3. MSEV genes found in scaffolds and predictions: Gene predictions from genome assembly scaffolds and AUGUSTUS gene predictions were searched for MSEV genes using tBLASTn. Results better than %ID >70%, E-value < $1x10^{-50}$, and query coverage > 70% were retained.

945